Structures, Energetics, and Vibrational Frequencies of Microhydrated Hexafluorophosphate, $PF_6^-(H_2O)_{n=1,2}$ from DFT and Ab Initio Computations

by

Yasmeen A. Abdo

A thesis submitted to the faculty of The University of Mississippi in partial fulfillment of the requirements of the Sally McDonnell Barksdale Honors College.

Oxford

May 2019

Approved by

Advisor: Dr. Gregory S. Tschumper

Reader: Dr. Ryan C. Fortenberry

Reader: Dr. Nathan I. Hammer

Acknowledgements

I would like to thank Dr.Tschumper for allowing me to work in his lab during my years as an undergraduate. In addition, I would like to thank the Tschumper group, especially Dr.Thomas Sexton, Sarah Johnson, Alex Denette, Caroline Radar, and Carly Rock, for their indispensable support and assistance. I would like to thank the faculty and staff of the Sally McDonnell Barksdale Honors College, especially Dr.Debra Young, for their dedication to our education. I would like to thank the Department of Chemistry and Biochemistry, especially Dr.Susan Pedigo and Dr.Walter Cleland. Finally, I would like to thank my readers, Dr.Ryan Fortenberry and Dr.Nathan Hammer. This work was done using computational resources from the Mississippi Center for Supercomputing Research and funding from the National Science Foundation (CHE-1338056, CHE-1664998).

Abstract

This study systematically examines an anion commonly used in room temperature ionic liquids, hexafluorophosphate PF_6^-, and its non-covalent interactions with up to two explicit water molecules ($PF_6^-(H_2O)_n$ where n = 1, 2). Initial low-energy configurations are identified via a set of relaxed angular scans across the edges and faces of the PF_6^- octahedron using the global hybrid M06-2X density functional with a triple-ζ correlation consistent basis set augmented with diffuse functions on all non-hydrogen atoms (cc-pVTZ for H and aug-cc-pVTZ for P, O, F; denoted haTZ). Full geometry optimizations are performed on these initial structures using a variety of common density functionals theory (DFT) methods (B3LYP, B3LYP-D3, M06-2X, and ωB97XD) as well as the MP2 and CCSD(T) *ab initio* methods with the same haTZ basis set. The corresponding harmonic vibrational frequencies are computed for all identified stationary points. Single point energy computations are also performed on the CCSD(T)/haTZ geometries using the CCSD(T) method with an analogous quadruple-ζ basis set (haQZ). A new $PF_6^-(H_2O)_2$ minimum has been identified that is approximately 2 kcal mol^{-1} lower in energy than any other structure previously reported in the literature. For the $PF_6^-(H_2O)_1$ system, DFT computations identify two unique stationary points competing for the lowest energy configuration, which is consistent with prior work. However, only one of these structures is a stationary point on the MP2 and CCSD(T) potential energy surfaces. This result suggests that some DFT methods might not correctly describe the interaction between $PF_6^-$and H_2O.

Contents

1 Introduction

Room Temperature Ionic Liquids (RTILs) are ionic salts that form liquids at or near room temperature.[1] RTILs are increasingly used as solvents in a wide range of applications because of their low vapor pressures, high conductivities, and low flammability. In addition, by changing the anion-cation combination or adding a co-solvent, the properties of the RTIL can be customized for particular application.[1]

Water, a common co-solvent and potential impurity, has the potential to change the physical properties of a given RTIL (*e.g.* conductivity, density, solubility, viscosity).[2–4] The water-RTIL interaction has been studied extensively in the literature both experimentally and computationally. Studies have found that when compared to the cation-water interaction, the anion-water interactions contributed more to the strength of water's interaction with an RTIL.[5–9] In addition, several studies found that the anion and water form an alternating Anion-Water-Anion pattern when interacting.[4,5,10,11]

Compared to other commonly used RTILs, the PF_6^- based RTILs have been shown to form some of the weakest water-anion hydrogen bonds[5] and have one of the lowest miscibilities with water.[7,12–14] As such, PF_6^- is one of the least hygroscopic anions for RTILs, and is generally used to make "hydrophobic" ionic liquids.[15]

In order to get a more detailed understanding of the water-anion interaction in PF_6^- based RTILs, two studies focused on the explicit solvation of PF_6^- with one or two water molecules ($PF_6^-(H_2O)_{n=1,2}$) and without the presence of a cation.[15,16] Wang *et al.* identified a monohydrate structure (denoted as configuration C_{2v} Edge in Figure 1 of the present study) as well as a dihydrate configuration (denoted as configuration D_{2h} Edge-Edge in Figure 2 of the present study).[15] In that study, these structures were identified as minima on the HF/6-31G* potential energy surfaces but

not with the B3LYP or MP2 methods when using the same 6-31G* basis set. In response to Wang *et al.*, Rodriguez-Otero *et al.* published a subsequent analysis that was able to identify the corresponding minima with both the B3LYP and MP2 methods when using the 6-31++G** basis set.[16] In addition, Rodriguez-Otero *et al.* identified another monohydrate water structure (denoted as configuration C_s Edge in Figure 1 of the present study), but only when they did not include diffuse functions in their basis sets. This present study builds upon these prior works by performing a more extensive exploration of the possible configurations for the $PF_6{}^-(H_2O)_{n=1,2}$ systems using both DFT and *ab initio* methods.

2 Computational Methods

Relaxed angular scans are performed over several coordinates of $PF_6^-(H_2O)_n$ (where n = 1,2) using the M06-2X[17] density functional with Dunning's correlation consistent triple-ζ basis set augmented with diffuse functions on all non-hydrogen atoms (cc-pVTZ for H and aug-cc-pVTZ for P ,O, and F; denoted haTZ).[18,19] The resulting low-energy configurations are then fully optimized with the haTZ basis set using various density functional theory (DFT) methods (B3LYP[20], B3LYP-D3[20,21], M06-2X, ωB97XD[22]) as well as the MP2[23] and CCSD(T)[24] *ab initio* methods. All optimizations are computed using analytical gradients. DFT harmonic vibrational frequencies are computed analytically for each stationary point whereas the CCSD(T) Hessians are obtained from the finite difference of analytical gradients. To validate the finite difference procedure, MP2 frequencies are computed both analytically and from the finite difference of analytical gradients (the two methods never differed by more than 1.0 cm^{-1}. Single point energy computations with the CCSD(T) methods and the corresponding haQZ basis set are performed on the CCSD(T)/haTZ geometries using `Molpro`. All DFT computations are performed with the `Gaussian09`[25] software package with a dense pruned numerical integration grid composed of 175 radical shells and 974 angular points per shell for H, O, and F and 250 radial shells with 974 angular points per shell for P corresponding to the superfine keyword in `Gaussian09`. MP2 computations are performed using both `Gaussian09` and `CFOUR`, whereas the CCSD(T) computations are performed with `CFOUR`.[26] All electronic energies are performed with pure angular momentum ($5d$ and $7f$) atomic orbital basis functions.

3 Results and Discussion

3.1 Structures and Energetics

Figure 1 and Figure 2 depict the mono- and dihydrate configurations of the $PF_6^-(H_2O)_n$ systems, respectively, along with selected intermolecular bond lengths. Configurations C_{2v} Edge, C_s Edge, and D_{2h} Edge-Edge have been previously reported.[15,16] The remaining unreported configurations included in Figures 1 and 2 originate from a set of relaxed angular scans performed with one or two water molecules on the faces and/or edges of the PF_6^- octahedron. All low-energy mono- and dihydrate configurations identified on the M06-2X/haTZ potential energy surface are fully optimized at the MP2/haTZ, then at the CCSD(T)/haTZ levels of theory. At the CCSD(T) and MP2 levels of theory, several of the initial M06-2X structures collapse to the configurations shown in Figures 1 and 2. These CCSD(T)/haTZ structures remain in similar geometries when optimized using the same basis set with the B3LYP, B3LYP-D3, M06-2X, ωB97XD, and MP2 methods.

For most configurations shown in Figure 1 and 2, either Edge and/or Face hydrogen bonds are observed. The Edge designation denotes the interaction of a water molecule with the two fluorine atoms along an edge of the PF_6^- octahedron while the Face designation denotes the interaction between a water molecule and the three fluorine atoms at the vertices of a face on the PF_6^- octahedron. The instances that involve high symmetry result in equivalent Edge and Face hydrogen bonds. Furthermore, the Face hydrogen bonds are usually shorter than the Edge hydrogen bonds. The C_s WW-Edge-Face configuration differs from the other structures in that the configuration contains a water-water hydrogen bond ($OH\cdots O$), and its Edge hydrogen bonds are shorter than its Face hydrogen bonds. In addition, the C_s WW-Edge-Face

configuration as a whole exhibits 1 OH···O interaction and 3 OH···F interactions, whereas all other structures exhibit either 2 or 4 OH···F interactions and no OH···O interactions.

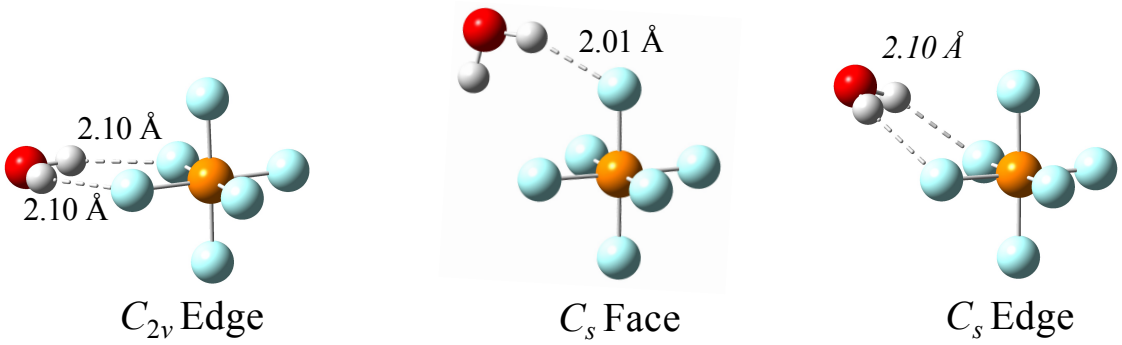

Figure 1: Optimized $PF_6^-(H_2O)_1$ configurations and intermolecular bond lengths at the CCSD(T)/haTZ level of theory (M06-2X/haTZ for the C_s Edge configuration).

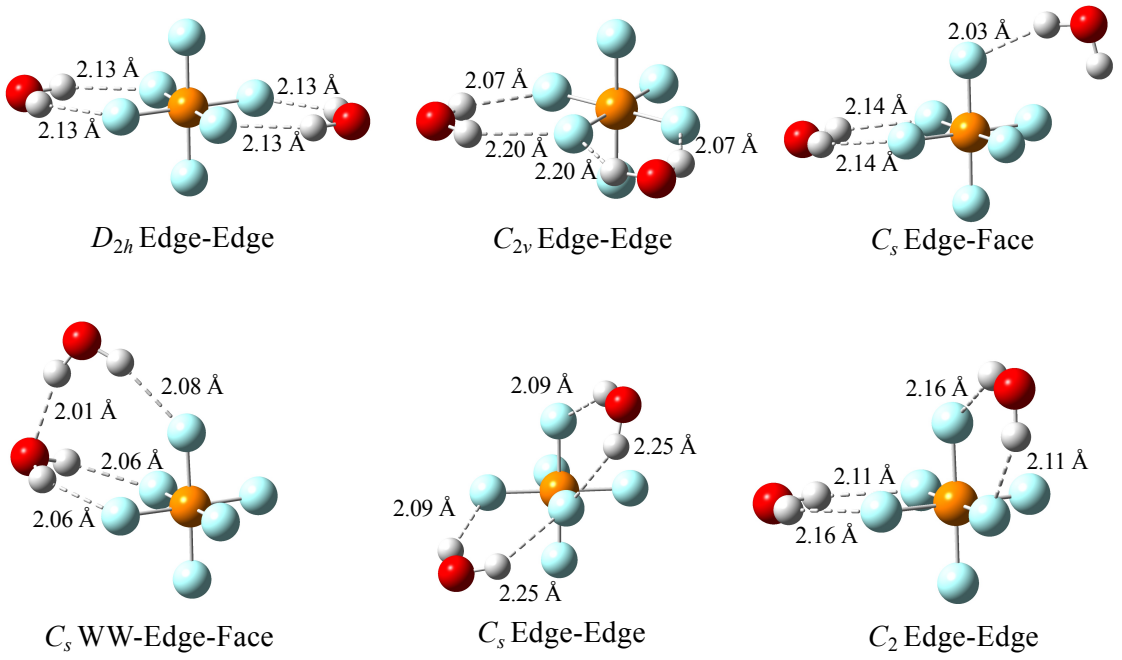

Figure 2: Optimized $PF_6^-(H_2O)_2$ configurations and intermolecular bond lengths at the CCSD(T)/haTZ level of theory

Table 1 reports the relative energetics (ΔE) and the number of imaginary modes

(n_i) assigned to each configuration in Figure 1 and 2, calculated from both DFT and *ab initio* methods. For the monohydrate system, CCSD(T) predicts the C_{2v} Edge configuration to be a minimum, while the C_s Face configuration is predicted to be a transition state that is +0.33 kcal mol^{-1} higher in energy. MP2 both qualitatively and quantitatively agrees with the CCSD(T) results. While the DFT methods all agree qualitatively that the C_{2v} Edge configuration is the lowest in energy, the predicted difference in energy between the two configurations ranges from +0.06 kcal mol^{-1} to +0.53 kcal mol^{-1}.

Furthermore, despite the qualitative energetic consistency with CCSD(T), the M06-2X and ωB97XD DFT methods differ from CCSD(T) in their assignment of imaginary modes. M06-2X assigns the C_{2v} Edge configuration as a transition state while ωB97XD not only assigns the C_{2v} Edge configuration as a transition state, but also assigns the higher energy C_s Face configuration as a minimum.

Table 1: Relative electronic energies (ΔE in kcal mol^{-1}) and number of imaginary modes (n_i) of the $PF_6^-(H_2O)_{n=1,2}$ configurations at various methods with the haTZ basis set as well as the CCSD(T)/haQZ energy points using the CCSD(T)/haTZ geometries.

		CCSD(T)		MP2	B3LYP	B3LYP-D3	ωB97XD	M06-2X
Structure		haQZ	haTZ	haTZ	haTZ	haTZ	haTZ	haTZ
C_{2v} Edge	ΔE	+0.00	+0.00	+0.00	+0.00	+0.00	+0.00	+0.00
	n_i	–	0	0	0	0	1	1
C_s Face	ΔE	+0.38	+0.33	+0.34	+0.53	+0.47	+0.15	+0.06
	n_i	–	1	1	1	1	0	1
D_{2h} Edge-Edge	ΔE	+0.00	+0.00	+0.00	+0.00	+0.00	+0.00	+0.00
	n_i	–	0	0	0	0	3	2
C_s WW-Edge-Face	ΔE	−2.09	−2.09	−2.11	−1.95	−2.36	−2.48	−2.29
	n_i	–	0	0	0	0	0	0
C_s Edge-Edge	ΔE	+0.38	+0.30	+0.35	+0.50	+0.37	+0.22	+0.04
	n_i	–	0	0	0	0	0	0
C_2 Edge-Edge	ΔE	+0.08	+0.08	+0.01	+0.01	+0.01	+0.00	−0.18
	n_i	–	0	0	0	0	0	0
C_s Edge-Face	ΔE	+0.37	+0.31	+0.32	+0.47	+0.41	+0.16	−0.04
	n_i	–	1	1	1	1	1	1
C_{2v} Edge-Edge	ΔE	+0.30	+0.29	+0.28	+0.27	+0.27	+0.30	+0.36
	n_i	–	1	1	0	1	1	0

Figure 3 depicts the relaxed angular scan used to rationalize the predictions of the M06-2X and ωB97XD methods. The relaxed angular scan explores the relationship between C_{2v} Edge, C_s Face, and C_s Edge configurations on various potential energy surfaces. The C_s Edge configuration is previously reported to be the monohydrate

minimum only when the $PF_6^-(H_2O)_1$ system is optimized using the B3LYP and MP2 methods with a double-ζ basis set and no added diffuse functions.[16] The scan, which is performed with the haTZ basis set, shows that the C_s Edge configuration is predicted to be the lowest energy minimum only on the M06-2X and ωB97XD potential energy surfaces and not along the B3LYP, B3LYP-D3, MP2, or CCSD(T) potential energy surfaces. Because this structure does not exist at higher levels of theory, results for the C_s Edge configuration have been relegated to the Supporting Information (SI) along with a handful of other mono- and dihydrate configurations that only appear as stationary points on the M06-2X/haTZ potential energy surface.

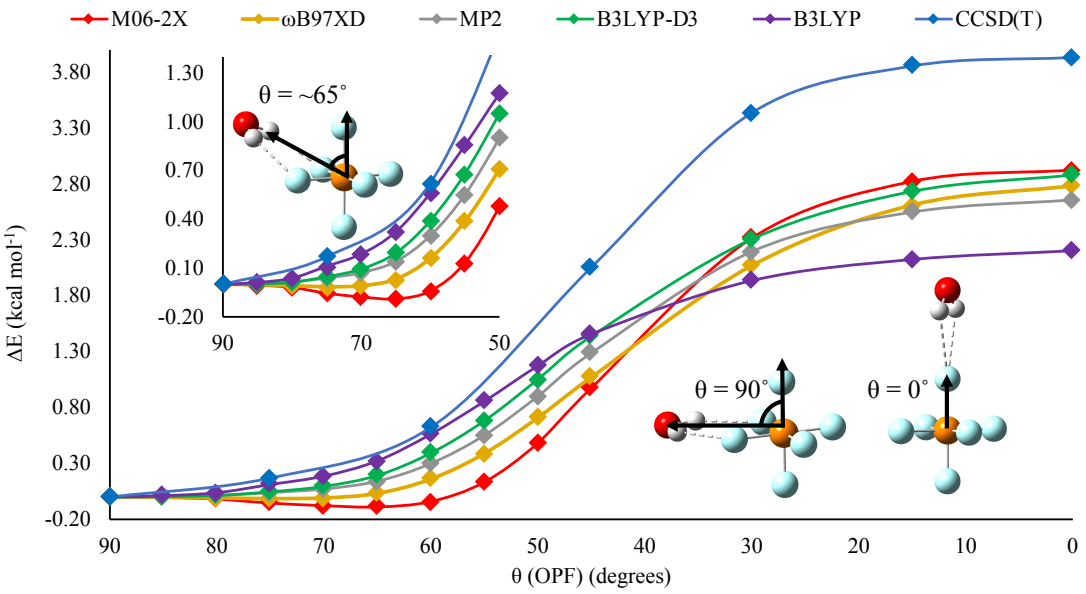

Figure 3: Relaxed C_s scans using the haTZ basis set of an H_2O molecule along a face of PF_6^- where the scan angle, θ(OPF), is 90° for the C_{2v} Edge configuration and ~65° for the C_s Edge configuration.

For the dihydrate system, CCSD(T) predicts four minimum configurations (D_{2h} Edge-Edge, C_s WW-Edge-Face, C_s Edge-Edge, and C_2 Edge-Edge) and two transition state configurations (C_s Edge-Face and C_{2v} Edge-Edge). The n_i for C_s WW-Edge-Face,C_s Edge-Edge, C_2 Edge-Edge, and C_s Edge-Face are based on the CCSD(T)/heavy-

aug-cc-pVDZ computations. The CCSD(T)/haTZ frequency computations are currently in progress. Almost isoenergetic to the D_{2h} Edge-Edge configuration, the literature minimum, is the C_2 Edge-Edge configuration which is only about +0.08 kcal mol^{-1} higher in energy. The two transition state configurations, C_s Edge-Face and C_{2v} Edge-Edge as well as the minimum C_s Edge-Edge configuration are all around +0.3 kcal mol^{-1} higher in energy than the D_{2h} Edge-Edge configuration. The CCSD(T) relative energetics presented in the current study predict the C_s WW-Edge-Face structure to be lower in energy than the previously reported lowest energy configuration, D_{2h} Edge-Edge, by 2 kcal mol^{-1}. The energy difference may stem from the stabilizing power of the OH$\cdots$O interaction present only in the C_s WW-Edge-Face configuration.

Most of the MP2 and DFT methods agree with the relative energetics of the configurations predicted by CCSD(T). However, though M06-2X predicts the C_s WW-Edge-Face configuration to be the lowest energy configuration by around 2 kcal mol^{-1}, the method disagrees with CCSD(T) on the relative energies of the higher energy configurations.

Several DFT methods disagree with the characterization of the configurations on the CCSD(T) potential energy surfaces. ωB97XD predicts the D_{2h} Edge-Edge configuration to be a higher order stationary point with three imaginary modes. In addition to predicting the D_{2h} Edge-Edge configuration to be a higher order stationary point with two imaginary modes, M06-2X also predicts the C_{2v} Edge-Edge configuration to be a minimum, rather than a transition state. Finally, B3LYP assigns the C_{2v} Edge-Edge configuration to be a minimum rather than a transition state.

Table 2 reports the dissociation energies (D_e) for the minimum configurations of both the mono- and dihydrate systems. The monohydrate configuration, C_{2v} Edge is fairly well bound, with a dissociation energy of 10.67 kcal mol^{-1}. DFT and MP2 are consistent with CCSD(T) in that they also predict a D_e of around 10 kcal mol^{-1} for the monohydrate system. For the dihydrate system, the C_s WW-Edge-Face configu-

ration has the highest dissociation energy around 22 kcal mol^{-1} while the other three minimum configurations, D_{2h} Edge-Edge, C_s Edge-Edge, and C_2 Edge-Edge all have dissociation energies around 20 kcal mol^{-1}. While both DFT and MP2 qualitatively agree with the CCSD(T) prediction, B3LYP quantitatively underestimates the D_e by around 3 kcal mol^{-1}.

Table 2: Dissociation energies (D_e in kcal mol^{-1}) of the $PF_6{}^-(H_2O)_{n=1,2}$ configurations at various methods with the haTZ basis set as well as the CCSD(T)/haQZ energy points using the CCSD(T)/haTZ geometries indicated in parentheses.

	CCSD(T)		MP2	B3LYP	B3LYP-D3	ωB97XD	M06-2X
Structure	haQZ	haTZ	haTZ	haTZ	haTZ	haTZ	haTZ
C_{2v} Edge	10.55	10.67	10.44	9.16	10.68	10.22	11.00
D_{2h} Edge-Edge	20.17	20.43	19.96	17.43	20.41	19.53	21.00
C_s WW-Edge-Face	22.26	22.52	22.07	19.38	22.78	22.02	23.29
C_s Edge-Edge	19.80	20.10	19.61	16.92	20.04	19.31	20.96
C_2 Edge-Edge	20.09	20.35	19.95	17.41	20.40	19.53	21.18

In order to asses the effects of the inconsistencies produced by the basis set super position error (BSSE)[27,28], the Boys-Bernardi counterpoise correction procedure[29,30] is applied to the lowest energy minimum of each system. Table 3 reports both the uncorrected and counterpoise corrected dissociation energies for the lowest energy monohydrate minimum, C_{2v} Edge, and the lowest energy dihydrate minimum, C_s WW-Edge-Face. The gap between the corrected and uncorrected dissociation energies is 0.6 kcal mol^{-1} for the C_{2v} Edge configuration according to CCSD(T)/haTZ. This gap between the uncorrected and corrected D_e shrinks as expected when computed using the CCSD(T)/haQZ energy point, which predicts the gap to be 0.27 kcal mol^{-1}. While MP2 agrees with both CCSD(T) results, DFT underestimates the BSSE and predicts the gap between the uncorrected and corrected dissociation

energies to be around 0.2 kcal mol^{-1}. The BSSE increases when computed for the dihydrate system. CCSD(T)/haTZ and the CCSD(T)/haQZ energy points predict a BSSE of 1.4 kcal mol^{-1} and 0.59 kcal mol^{-1} respectively. While MP2 is consistent with these predictions, DFT again underestimates the BSSE, predicting it to be around 0.4 kcal mol^{-1}.

Table 3: Uncorrected (D_e in kcal mol^{-1}) and counterpoise corrected (D_e^{cp} in kcal mol^{-1}) dissociation energies for the lowest energy monohydrate structure C_{2v} Edge, and the lowest energy dihydrate configuration, C_s WW-Edge-Face, at various methods with the haTZ basis set as well as the CCSD(T)/haQZ energy points using the CCSD(T)/haTZ geometries.

	C_{2v} Edge		C_s WW-Edge-Face	
Method	D_e	D_e^{cp}	D_e	D_e^{cp}
CCSD(T)/haQZ	10.55	10.28	22.26	21.67
CCSD(T)/haTZ	10.67	10.06	22.52	21.12
MP2/haTZ	10.44	9.85	22.07	20.71
B3LYP/haTZ	9.16	8.95	19.38	18.99
B3LYP-D3/haTZ	10.68	10.49	22.78	22.37
ωB97XD/haTZ	10.22	10.03	22.02	21.61
M06-2X/haTZ	11.00	10.83	23.29	22.89

3.2 Vibrational Frequencies

Table 4 reports the frequency shifts ($\Delta\omega$ in cm^{-1}) of the mono- and dihydrate configurations' symmetric and asymmetric water stretches relative to the reported isolated water monomer's symmetric (a_1) and asymmetric (b_2) frequencies. The CCSD(T) frequency calculations for the C_s WW-Edge-Face, C_s Edge-Edge, and C_2 Edge-Edge are currently in progress. For the C_{2v} Edge configuration, when the complexed wa-

ter is stretching symmetrically, the shift is taken relative to the symmetric stretch frequency of an isolated water monomer and is found to be -17 cm^{-1}. The analogous method is used to calculate the shift of the asymmetric stretch in the C_{2v} Edge configuration which is found to be -72 cm^{-1}.

Table 4: Harmonic vibrational frequencies for the symmetric (a_1) and asymmetric (b_2) stretches of an isolated water molecule (ω in cm^{-1}) and the Frequency shifts ($\Delta\omega$ in cm^{-1}) of the complexed water relative to the former, all computed using the haTZ basis set.

Structure	H_2O Ref.	CCSD(T)	MP2	B3LYP	B3LYP-D3	ωB97XD	M06-2X
H_2O							
$\omega(a_1)$	–	3814	3825	3801	3801	3882	3872
$\omega(b_2)$	–	3924	3952	3904	3904	3989	3976
C_{2v} Edge							
$\Delta\omega(a_1)$	a_1	−17	−27	−27	−27	−32	−28
$\Delta\omega(b_2)$	b_2	−72	−86	−83	−87	−90	−87
D_{2h} Edge-Edge							
$\Delta\omega(b_{3u})$	a_1	−13	−22	−22	−22	−26	−24
$\Delta\omega(a_g)$	a_1	−12	−22	−21	−21	−26	−23
$\Delta\omega(b_{1g})$	b_2	−63	−76	−73	−76	−80	−77
$\Delta\omega(b_{2u})$	b_2	−62	−75	−72	−75	−79	−76
C_s WW-Edge-Face							
$\Delta\omega(a')$	a_1		−118	−140	−138	−219	−94
$\Delta\omega(a')$	a_1		−48	−47	−47	−128	−49
$\Delta\omega(a')$	b_2		−118	−106	−114	−199	−117
$\Delta\omega(a'')$	b_2		−110	−105	−109	−195	−107
C_s Edge-Edge							
$\Delta\omega(a'')$	a_1		−26	−37	−24	−32	−25
$\Delta\omega(a')$	a_1		−24	−35	−23	−31	−24
$\Delta\omega(a'')$	b_2		−72	−61	−71	−72	−75
$\Delta\omega(a')$	b_2		−69	−58	−67	−69	−72
C_2 Edge-Edge							
$\Delta\omega(b)$	a_1		−23	−22	−22	−27	−25
$\Delta\omega(a)$	a_1		−22	−22	−21	−26	−24
$\Delta\omega(a)$	b_2		−76	−72	−75	−79	−76
$\Delta\omega(b)$	b_2		−75	−71	−75	−78	−75

For the dihydrate D_{2h} Edge-Edge, C_s Edge-Edge, and C_2 Edge-Edge configurations, highly coupled vibrational modes between the two water molecules are observed. For any given water stretch, both water molecules are stretching either symmetrically or asymmetrically with respect to the individual water molecule, regardless of the overall symmetry of the configuration. The shift for the water's symmetric stretch for these dihydrate systems is found to be 20-30 cm^{-1}, while the shift for the asymmetric stretch is found to be 70-80 cm^{-1}.

However, the presence of the water-water hydrogen bond within the C_s WW-Edge-Face configuration affects the overall frequency shifts. This can be seen in the dramatic difference between the two symmetric shifts, where a -118 cm^{-1} shift is observed when the hydrogen bond donor O-H stretch has a larger amplitude than the acceptor water molecule's symmetric stretching. When both water molecules have similar stretching amplitudes, a frequency shift of -48 cm^{-1} is observed. The asymmetric stretches are not as highly coupled as the symmetric stretches resulting in separate asymmetric stretching shifts for the hydrogen bond donor (-118 cm^{-1}) and the acceptor (-110 cm^{-1}). The MP2 shifts are reported here and will be updated when the CCSD(T) computations finish.

4 Conclusions

Low energy configurations of the $PF_6^-(H_2O)_{n=1,2}$ system are identified via a set of relaxed angular scans across the edges and faces of the PF_6^- octahedron. Two low lying stationary points are found for the $PF_6^-(H_2O)_1$ system by the DFT methods; however, only configuration C_{2v} Edge is found with the MP2 and CCSD(T) *ab initio* methods. Additionally, the identification of C_{2v} Edge as the minimum for the $PF_6^-(H_2O)_1$ system is in agreement with the previous literature.[15,16] For the $PF_6^-(H_2O)_2$ system, four minima and two transition states are identified, with the lowest energy minimum being approximately 2 kcal mol^{-1} lower than any other structure identified in the current study or in previous literature. Though the previously reported D_{2h} Edge-Edge configuration is identified, the lower energy C_s WW-Edge-Face configuration found agrees with what is already known about the hydration of PF_6^- with only 2 H_2Omolecules: the water$\cdots$water interactions are already competitive the OH$\cdots$F interactions in the system.[14] In conclusion, MP2 consistently agrees with the CCSD(T) benchmarks for energetics. The M06-2X and ωB97XD methods disagree with the CCSD(T) characterization of structures as minima or transition states. An in-depth frequency analysis that will be conducted once the CCSD(T) frequency computations finish will allow further comparison beteween DFT and *ab initio* methods.

References

[1] R. D. Rogers and K. R. Seddon, *Science*, **302**, 792 (2003). Ionic Liquids-Solvents of the Future. http://dx.doi.org/10.2307/3835533.

[2] K. R. Seddon, A. Stark, and M.-J. Torres, *Pure Appl. Chem.*, **72**, 2275 (2000). Influence of chloride, water, and organic solvents on the physical properties of ionic liquids. http://dx.doi.org/10.1351/pac200072122275.

[3] L. A. Blanchard, Z. Gu, and J. F. Brennecke, *J. Phys. Chem. B*, **105**, 2437 (2001). High-Pressure Phase Behavior of Ionic Liquid/CO2 Systems. http://dx.doi.org/10.1021/jp003309d.

[4] Y. Danten, M. I. Cabaco, and M. Besnard, *J. Phys. Chem. A*, **113**, 2873 (2009). Interaction of Water Highly Diluted in 1-Alkyl-3-methyl Imidazolium Ionic Liquids with the PF- and BF- Anions. http://dx.doi.org/10.1021/jp8108368.

[5] L. Cammarata, S. G. Kazarian, P. Salter, and T. Welton, *Physical Chemistry Chemical Physics*, **3**, 5192 (2001). Molecular States of Water in Room Temperature Ionic Liquids. http://dx.doi.org/10.1039/B106900D.

[6] J. Schenk, U. Panne, and M. Albrecht, *J. Phys. Chem. B*, **116**, 14171 (2012). Interaction of Levitated Ionic Liquid Droplets with Water. http://dx.doi.org/10.1021/jp309661p.

[7] J. G. Huddleston, A. E. Visser, W. M. Reichert, H. D. Willauer, G. A. Broker, and R. D. Rogers, *Green Chemistry*, **3**, 156 (2001). Characterization and comparison of hydrophilic and hydrophobic room temperature ionic liquids incorporating the imidazolium cation. http://dx.doi.org/10.1039/B103275P.

[8] A. A. Niazi, B. D. Rabideau, and A. E. Ismail, *J. Phys. Chem. B*, **117**, 1378 (2013). Effects of Water Concentration on the Structural and Diffusion Properties of Imidazolium-Based Ionic LiquidWater Mixtures. http://dx.doi.org/10.1021/jp3080496.

[9] I. Khan, K. A. Kurnia, F. Mutelet, S. P. Pinho, and J. A. P. Coutinho, *J. Phys. Chem. B*, **118**, 1848 (2014). Probing the Interactions between Ionic Liquids and Water: Experimental and Quantum Chemical Approach. http://dx.doi.org/10.1021/jp4113552.

[10] A. R. Porter, S. Y. Liem, and P. L. A. Popelier, *Phys. Chem. Chem. Phys.*, **10**, 4240 (2008). Room temperature ionic liquids containing low water concentrationsa molecular dynamics study. http://dx.doi.org/10.1039/B718011J.

[11] C. G. Hanke, N. A. Atamas, and R. M. Lynden-Bell, *Green Chemistry*, **4**, 107 (2002). Solvation of small molecules in imidazolium ionic liquids: a simulation study. http://dx.doi.org/10.1039/B109179B.

[12] M. H. Ghatee and A. R. Zolghadr, *J. Phys. Chem. C*, **117**, 2066 (2013). Local Depolarization in Hydrophobic and Hydrophilic Ionic Liquids/Water Mixtures: CarParrinello and Classical Molecular Dynamics Simulation. http://dx.doi.org/10.1021/jp305334i5.

[13] R. P. Swatloski, A. E. Visser, W. M. Reichert, G. A. Broker, L. M. Farina, J. D. Holbrey, and R. D. Rogers, *Green Chemistry*, **4**, 81 (2002). On the solubilization of water with ethanol in hydrophobic hexafluorophosphate ionic liquids. http://dx.doi.org/10.1039/B108905F.

[14] C. G. Hanke and R. M. Lynden-Bell, *J. Chem. Phys. B*, **107**, 10873 (2003). A Simulation Study of Water-Dialkylimidazolium Ionic Liquid Mixtures. http://dx.doi.org/10.1021/jp034221d.

[15] Y. Wang, H. Li, and S. Han, *J. Phys. Chem. B*, **110**, 24646 (2006). A Theoretical Investigation of the Interactions between Water Molecules and Ionic Liquids. http://dx.doi.org/10.1021/jp064134w.

[16] J. Rodriguez-Otero, E. M. Cabaleiro-Lago, and A. Pena-Gallego, *J. Phys. Chem. B*, **112**, 13465 (2008). Comment on A Theoretical Investigation of the Interactions between Water Molecules and Ionic Liquids. http://dx.doi.org/10.1021/jp8052983.

[17] Y. Zhao and D. G. Truhlar, *Theoretical Chemistry Accounts*, **120**, 215 (2008). The M06 suite of density functionals for main group thermochemistry, thermochemical kinetics, noncovalent interactions, excited states, and transition elements: two new functionals and systematic testing of four M06-class functionals and 12 other functionals. http://dx.doi.org/10.1007/s00214-007-0401-8.

[18] T. H. Dunning, *J. Chem. Phys.*, **90**, 1007 (1989). Gaussian basis sets for use in correlated molecular calculations. I. The atoms boron through neon and hydrogen. http://dx.doi.org/10.1063/1.456153.

[19] R. A. Kendall, T. H. Dunning, and R. J. Harrison, *J. Chem. Phys.*, **96**, 6796 (1992). Electron affinities of the first-row atoms revisited. Systematic basis sets and wave functions. http://dx.doi.org/10.1063/1.462569.

[20] C. Lee, W. Yang, and R. G. Parr, *Phys. Rev. B*, **37**, 785 (1988). Development of the Colle-Salvetti correlation-energy formula into a functional of the electron density. http://dx.doi.org/10.1103/PhysRev.37.785.

[21] S. Grimme, J. Anthony, S. Ehrlich, and H. Krieg, *J. Chem. Phys.*, **132**, 154104 (2010). A consistent and accurate ab initio parameterization of density functional dispersion correction (DFT-D) for the 94 elements H-Pu. http://dx.doi.org/10.1063/1.3382344.

[22] J. Chai and M. Head-Gordon, *Phys. Chem. Chem. Phys.*, **10**, 6615 (2008). Long-range corrected hybrid density functionals with damped atom-atom dispersion corrections. http://dx.doi.org/10.1039/B810189B.

[23] C. Møller and M. S. Plesset, *Phys. Rev.*, **46**, 618 (1934). Note on an Approximation Treatment for Many-electron Systems. http://dx.doi.org/10.1103/PhysRev.46.618.

[24] R. J. Bartlett, *WIREs Comput. Mol Sci.*, **2**, 126 (2012). Coupled-cluster Theory and its Equation-of-motion Extensions. http://dx.doi.org/10.1002/wcms.76.

[25] M. J. Frisch, G. W. Trucks, H. B. Schlegel, G. E. Scuseria, M. A. Robb, J. R. Cheeseman, G. Scalmani, V. Barone, B. Mennucci, G. A. Petersson, H. Nakatsuji, M. Caricato, X. Li, H. P. Hratchian, A. F. Izmaylov, J. Bloino, G. Zheng, J. L. Sonnenberg, M. Hada, M. Ehara, K. Toyota, R. Fukuda, J. Hasegawa, M. Ishida, T. Nakajima, Y. Honda, O. Kitao, H. Nakai, T. Vreven, Montgomery Jr., J. A., J. E. Peralta, F. Ogliaro, M. Bearpark, J. J. Heyd, E. Brothers, K. N. Kudin, V. N. Staroverov, R. Kobayashi, J. Normand, K. Raghavachari, A. Rendell, J. C. Burant, S. S. Iyengar, J. Tomasi, M. Cossi, N. Rega, J. M. Millam, M. Klene, J. E. Knox, J. B. Cross, V. Bakken, C. Adamo, J. Jaramillo, R. Gomperts, R. E. Stratmann, O. Yazyev, A. J. Austin, R. Cammi, C. Pomelli, J. W. Ochterski, R. L. Martin, K. Morokuma, V. G. Zakrzewski, G. A. Voth, P. Salvador, J. J. Dannenberg, S. Dapprich, A. D. Daniels, O. Farkas, J. B. Foresman, J. V. Ortiz, J. Cioslowski, and D. J. Fox, gaussian Inc. Wallingford CT 2009. Gaussian09 Revision D.01.

[26] J. F. Stanton, J. Gauss, M. E. Harding, and P. G. Szalay, with contributions from A.A. Auer and R.J. Bartlett and U. Benedikt and C. Berger and D.E. Bernholdt and Y.J. Bomble and L. Cheng and O. Christiansen and M. Heckert and O. Heun and C. Huber and T.-C. Jagau and D. Jonsson and J. Jusélius and

K. Klein and W.J. Lauderdale and D.A. Matthews and T. Metzroth and L.A. Mück and D.P. O'Neill and D.R. Price and E. Prochnow and K. Ruud and F. Schiffmann and W. Schwalbach and S. Stopkowicz and A. Tajti and J. Vázquez and F. Wang and J.D. Watts and the integral packages MOLECULE (J. Almlöf and P.R. Taylor) and PROPS (P.R. Taylor) and ABACUS (T. Helgaker and H.J. Aa. Jensen and P. Jørgensen and J. Olsen) and ECP routines by A. V. Mitin and C. van Wüllen. For the current version see http://www.cfour.de. CFOUR, Coupled-Cluster techniques for Computational Chemistry.

[27] N. R. Kestner, *J. Chem. Phys.*, **48**, 252 (1968). He-He Interaction in the SCF-MO Approximation. http://dx.doi.org/10.1063/1.1667911.

[28] B. Liu and A. D. McLean, *J. Chem. Phys.*, **59**, 4557 (1973). Accurate Calculation of the Attractive Interaction of Two Ground State Helium Atoms. http://dx.doi.org/10.1063/1.1680654.

[29] S. F. Boys and F. Bernardi, *Mol. Phys.*, **19**, 553 (1970). The Calculation of Small Molecular Interactions by the Differences of Separate Total Energies. Some Procedures with Reduced Errors. http://dx.doi.org/10.1080/00268977000101561.

[30] S. Simon, M. Duran, and J. J. Dannenberg, *J. Chem. Phys.*, **105**, 11024 (1996). How does Basis Set Superposition Error Change the Potential Surfaces for Hydrogen-bonded Dimers? http://dx.doi.org/10.1063/1.472902.

Appendix

Table A1: Harmonic vibrational frequencies (ω) and IR intensities for H_2O using the haTZ basis set.

	CCSD(T)		MP2		B3LYP		B3LYP-D3		ωB97XD		M06-2X	
Irrep	ω	IRIntensity	ω	IRIntensity	ω	IRIntensity	ω	IRIntensity	ω	IRIntensity	ω	IRIntensity
a_1	1648	72	1630	74	1628	77	1628	77	1638	79	1619	84
a_1	3814	5	3825	8	3801	6	3801	6	3882	6	3872	12
b_2	3924	55	3952	76	3904	63	3904	63	3989	64	3976	83

Table A2: Harmonic vibrational frequencies (ω) and IR intensities for PF_6^- using the haTZ basis set.

	CCSD(T)		MP2		B3LYP		B3LYP-D3		ωB97XD		M06-2X	
Irrep	ω	IR Intensity	ω	IR Intensity	ω	IR Intensity	ω	IR Intensity	ω	IR Intensity	ω	IR Intensity
a_u	302	0	300	0	292	0	292	0	298	0	294	0
e_u	302	0	300	0	292	0	292	0	298	0	294	0
e_u	302	0	300	0	292	0	292	0	298	0	294	0
t_{2g}	460	0	457	0	446	0	446	0	454	0	456	0
t_{2g}	460	0	457	0	446	0	446	0	454	0	456	0
t_{2g}	460	0	457	0	446	0	446	0	454	0	456	0
t_{1u}	550	61	547	30	536	26	537	26	545	28	546	34
t_{1u}	550	61	547	30	536	26	537	26	545	28	546	34
t_{1u}	550	61	547	30	536	26	537	26	545	28	546	34
e_g	574	0	568	0	546	0	546	0	562	0	577	0
e_g	574	0	568	0	546	0	546	0	562	0	577	0
a_{1g}	738	0	731	0	706	0	707	0	728	0	742	0
e_u	875	646	865	445	833	444	834	444	858	452	873	440
e_u	875	646	865	445	833	444	834	444	858	452	873	440
a_u	875	646	865	445	833	444	834	444	858	452	873	440

Table A3: Harmonic vibrational frequencies (ω) and IR intensities for the C_{2v} Edge configuration using the haTZ basis set.

	CCSD(T)		MP2		B3LYP		B3LYP-D3		ωB97XD		M06-2X	
Irrep	ω	IR Intensity	ω	IR Intensity	ω	IR Intensity	ω	IR Intensity	ω	IR Intensity	ω	IR Intensity
b_2	9	18	11	0	17	0	10	0	$11i$	0	$9i$	0
b_1	78	0	68	25	56	19	74	14	96	2	63	20
b_1	143	89	138	64	154	68	170	73	155	88	157	68
a_1	145	87	141	6	131	6	144	6	157	6	137	6
a_2	233	0	234	0	228	0	234	0	208	0	220	0
a_2	305	0	304	0	296	0	296	0	308	0	301	0
b_1	305	0	304	0	295	0	447	1	463	2	302	0
a_1	306	2	304	1	295	0	296	1	309	1	301	1
b_2	460	1	458	1	446	1	297	0	309	0	455	1
a_2	461	0	459	0	447	0	448	0	464	0	456	0
a_1	462	1	459	1	447	1	448	1	465	1	456	1
b_2	539	3	561	1	537	9	538	8	559	30	548	20
a_1	550	35	547	34	536	27	536	27	555	42	545	30
b_1	553	28	538	4	529	1	531	1	539	25	537	1
b_2	563	116	550	26	540	13	541	15	577	1	553	5
b_1	568	1	562	158	555	159	565	155	565	158	563	163
a_1	579	4	572	4	550	5	551	5	589	4	566	6
a_1	738	7	731	7	707	8	708	8	754	7	727	10
b_1	868	390	882	446	851	447	853	447	906	454	876	453
a_1	868	501	859	511	828	510	829	513	881	521	850	517
b_2	891	436	859	390	827	390	828	387	881	396	849	397
a_1	1696	119	1678	169	1682	179	1685	186	1677	190	1690	181
a_1	3797	69	3797	112	3774	101	3774	114	3844	131	3849	111
b_1	3852	42	3866	88	3821	79	3817	82	3890	103	3899	78

Table A4: Harmonic vibrational frequencies (ω) and IR intensities for the C_s Face configuration using the haTZ basis set.

	CCSD(T)		MP2		B3LYP		B3LYP-D3		ωB97XD		M06-2X	
Irrep	ω	IR Intensity	ω	IR Intensity	ω	IR Intensity	ω	IR Intensity	ω	IR Intensity	ω	IR Intensity
a''	$62i$	3	$55i$	3	$40i$	1	$60i$	3	11	0	$64i$	2
a'	58	3	55	3	38	2	55	2	74	1	73	1
a''	114	10	119	14	129	6	119	15	147	5	104	3
a'	138	6	135	6	140	27	141	6	152	12	153	5
a'	228	76	230	76	238	68	253	72	297	0	222	87
a''	301	0	299	0	290	0	290	0	300	0	303	0
a''	302	0	300	0	291	0	291	0	303	9	306	1
a'	311	2	309	2	300	3	302	4	323	75	313	1
a''	456	3	454	3	442	1	442	2	452	1	458	8
a'	462	0	460	0	448	1	448	1	457	0	466	0
a'	464	0	461	0	450	0	450	0	460	0	467	0
a''	509	60	514	51	521	21	516	31	521	44	499	73
a'	551	29	548	27	535	7	536	13	547	25	556	35
a''	552	59	549	61	538	33	538	53	548	36	557	60
a'	553	39	550	37	539	20	539	32	549	71	558	44
a'	569	3	562	4	539	62	540	15	559	4	580	2
a''	585	14	580	18	560	40	563	39	581	20	597	16
a'	738	4	731	4	707	6	708	5	733	3	754	4
a'	864	439	854	445	821	457	823	448	848	456	879	444
a'	883	450	874	453	845	446	845	450	876	458	896	467
a''	884	452	875	457	846	456	847	459	878	465	897	471
a'	1699	140	1681	137	1679	130	1685	147	1702	146	1677	171
a'	3779	129	3772	162	3721	227	3738	191	3824	153	3835	128
a'	3865	57	3885	68	3855	50	3847	50	3926	51	3899	80

Table A5: Harmonic vibrational frequencies (ω) and IR intensities for the D_{2h} Edge-Edge configuration using the haTZ basis set.

	CCSD(T)		MP2		B3LYP		B3LYP-D3		ωB97XD		M06-2X	
Irrep	ω	IR Intensity	ω	IR Intensity	ω	IR Intensity	ω	IR Intensity	ω	IR Intensity	ω	IR Intensity
b_{1u}	8	1	9	1	12	1	7	1	$3i$	1	$9i$	1
b_{2g}	9	0	12	0	20	0	10	0	$9i$	0	$14i$	0
b_{2u}	55	15	49	24	39	21	52	14	$23i$	77	64	4
b_{1g}	91	0	77	0	62	0	87	0	34	0	114	0
a_g	133	0	129	0	118	0	132	0	133	0	143	0
b_{2u}	134	157	126	153	143	153	161	159	101	99	146	175
b_{1g}	142	0	139	0	153	0	168	0	127	0	144	0
b_{3u}	145	12	141	12	129	12	145	13	145	13	157	12
a_u	220	0	221	0	216	0	222	0	205	0	195	0
b_{3g}	225	0	225	0	220	0	227	0	209	0	199	0
a_u	308	0	306	0	298	0	299	0	304	0	310	0
b_{2u}	308	0	306	0	297	1	299	1	304	0	311	0
b_{3u}	309	2	307	2	298	2	300	2	304	2	313	3
b_{2g}	460	0	458	0	447	0	447	0	455	0	462	0
b_{3g}	463	0	460	0	448	0	449	0	458	0	466	0
a_g	463	0	460	0	447	0	450	0	458	0	467	0
b_{1u}	518	134	519	121	513	103	519	56	522	113	515	165
b_{2g}	529	0	530	0	525	0	536	0	533	0	525	0
b_{3u}	550	41	547	40	536	33	536	33	545	40	555	49
b_{2u}	556	24	553	23	540	20	542	19	553	22	562	26
b_{1u}	558	172	555	185	545	204	551	243	555	197	562	176
b_{1g}	566	0	560	0	537	0	538	0	564	0	576	0
a_g	584	0	577	0	555	0	556	0	574	0	595	0
a_g	741	0	734	0	709	0	711	0	736	0	757	0
b_{2u}	858	341	849	344	817	345	818	339	858	351	870	348
b_{3u}	860	595	850	600	819	601	819	608	859	611	872	617
b_{1u}	905	438	896	443	865	446	868	445	886	451	921	452
b_{3u}	1691	335	1672	334	1676	354	1679	368	1682	364	1670	377
a_g	1696	0	1677	0	1681	0	1684	0	1688	0	1675	0
b_{3u}	3801	174	3802	201	3779	179	3779	204	3855	203	3848	239
a_g	3801	0	3803	0	3780	0	3780	0	3856	0	3849	0
b_{1g}	3861	0	3876	0	3831	0	3828	0	3909	0	3899	0
b_{2u}	3862	136	3877	167	3832	150	3829	155	3910	148	3900	196

Table A6: Harmonic vibrational frequencies (ω) and IR intensities for the C_s WW-Edge-Face configuration using the haTZ basis set.

	CCSD(T)		MP2		B3LYP		B3LYP-D3		ωB97XD		M06-2X	
Irrep	ω	IR Intensity	ω	IR Intensity	ω	IR Intensity	ω	IR Intensity	ω	IR Intensity	ω	IR Intensity
a'			22	0	34	0	31	0	29	0	26	0
a''			26	2	29	3	28	2	31	1	27	1
a''			63	25	56	14	76	12	107	0	71	17
a'			93	1	77	1	96	1	114	1	99	1
a''			136	43	158	52	169	54	154	60	158	49
a'			156	13	147	13	160	13	165	10	157	13
a'			170	7	168	8	177	8	183	8	179	7
a''			297	3	290	1	291	1	265	36	294	4
a''			303	0	296	0	297	0	306	1	302	1
a'			307	1	298	1	300	1	315	1	305	1
a''			318	14	320	13	322	18	309	0	312	18
a'			384	21	382	20	398	17	386	22	400	18
a''			432	34	413	40	433	32	431	31	437	31
a''			458	1	447	0	448	4	465	1	456	2
a'			458	0	446	0	448	1	466	1	457	1
a'			463	2	451	2	453	2	470	1	460	2
a'			546	30	535	22	535	27	553	23	544	24
a'			548	32	536	30	537	27	557	50	546	33
a''			549	26	536	15	538	16	559	29	548	21
a''			564	1	542	9	543	8	579	0	557	5
a'			568	2	545	2	546	3	585	7	560	5
a'			636	218	634	213	647	213	628	254	651	225
a''			682	80	680	82	685	75	644	81	679	76
a'			731	15	706	16	707	17	754	14	726	21
a'			866	470	835	467	836	469	889	493	858	480
a''			867	394	835	396	837	395	890	405	859	402
a'			872	497	842	501	843	503	896	492	865	502
a'			1672	130	1676	128	1679	125	1661	94	1683	119
a'			1694	141	1693	165	1697	169	1686	188	1704	164
a'			3707	245	3661	271	3663	271	3778	212	3755	242
a'			3777	76	3754	84	3754	74	3823	38	3829	59
a'			3834	217	3799	167	3790	223	3860	326	3863	247
a''			3842	99	3798	92	3794	95	3869	113	3875	90

Table A7: Harmonic vibrational frequencies (ω) and IR intensities for the C_s Edge-Edge configuration using the haTZ basis set.

	CCSD(T)		MP2		B3LYP		B3LYP-D3		ωB97XD		M06-2X	
Irrep	ω	IR Intensity	ω	IR Intensity	ω	IR Intensity	ω	IR Intensity	ω	IR Intensity	ω	IR Intensity
a''			17	0	19	0	17	0	30	0	23	0
a'			20	1	21	1	23	1	27	0	21	1
a'			56	21	61	15	43	20	67	4	57	11
a''			56	6	63	5	31	3	83	2	64	3
a''			124	0	131	1	117	2	123	3	130	2
a'			135	5	139	4	126	7	138	34	133	3
a''			141	18	158	19	153	6	151	5	143	5
a'			143	105	167	105	163	116	149	4	155	67
a''			183	14	191	15	175	24	205	35	189	28
a'			210	17	220	18	209	13	219	101	206	68
a'			302	0	295	0	294	0	306	1	300	1
a''			303	1	296	1	296	1	306	1	300	1
a''			311	0	304	0	301	0	318	0	310	0
a'			454	6	444	3	444	4	456	25	451	7
a'			461	2	451	1	449	1	469	3	459	2
a''			461	0	451	0	449	0	469	0	459	0
a''			495	35	501	33	499	48	480	22	495	31
a'			517	115	521	56	520	67	499	141	513	123
a'			547	55	535	25	536	35	555	62	544	43
a''			552	61	542	64	540	64	560	64	550	58
a'			553	57	542	22	542	16	560	50	551	51
a'			563	19	547	132	543	106	581	20	557	32
a''			572	0	551	1	546	0	593	0	567	0
a'			730	15	707	19	706	17	754	13	726	19
a'			861	439	830	438	833	431	883	443	854	440
a'			873	439	844	443	839	453	897	452	865	448
a''			874	479	844	476	840	480	897	497	866	492
a''			1668	191	1674	198	1671	180	1667	240	1681	215
a'			1681	123	1688	148	1682	137	1680	117	1693	119
a''			3799	86	3777	75	3764	66	3847	122	3849	82
a'			3800	116	3778	128	3766	180	3848	88	3851	121
a''			3880	28	3833	36	3843	16	3901	45	3917	28
a'			3883	127	3837	104	3846	100	3905	138	3920	100

Table A8: Harmonic vibrational frequencies (ω) and IR intensities for the C_2 Edge-Edge configuration using the haTZ basis set.

	CCSD(T)		MP2		B3LYP		B3LYP-D3		ωB97XD		M06-2X	
Irrep	ω	IR Intensity	ω	IR Intensity	ω	IR Intensity	ω	IR Intensity	ω	IR Intensity	ω	IR Intensity
a			8	1	13	1	7	1	20	1	13	1
b			11	1	18	1	10	1	26	0	16	1
b			66	35	52	27	71	20	75	2	52	20
a			66	12	51	10	72	7	94	1	59	9
a			130	22	122	1	135	1	145	0	125	0
b			130	71	126	9	142	9	156	27	140	12
a			132	13	145	36	161	38	155	10	154	24
b			141	32	148	99	164	109	163	10	153	82
b			223	0	217	1	224	0	217	104	203	27
a			225	1	220	1	226	1	217	34	205	12
a			305	0	296	0	298	0	303	0	298	0
a			306	0	298	0	299	0	311	1	304	0
b			307	0	298	0	300	0	317	1	309	2
b			459	3	447	3	448	3	459	6	453	2
a			459	4	447	4	448	3	465	10	457	2
a			460	0	448	0	450	1	470	8	460	4
b			522	61	517	55	524	24	498	48	513	46
a			527	61	521	46	527	18	500	130	516	107
b			549	49	538	36	539	32	557	39	547	29
a			553	109	540	8	542	0	559	82	549	87
b			553	79	542	86	547	109	561	65	552	68
a			563	0	543	110	548	148	583	5	558	10
b			572	6	550	14	551	18	593	5	568	5
a			732	5	708	6	709	6	756	4	729	6
b			848	466	816	468	818	466	874	463	840	469
a			875	447	844	449	845	448	898	446	868	444
b			875	461	845	461	846	463	899	499	868	486
b			1671	265	1675	275	1678	293	1672	363	1684	336
a			1678	66	1681	75	1685	72	1678	4	1690	16
b			3802	153	3778	131	3779	156	3847	214	3855	179
a			3803	48	3779	51	3780	46	3848	2	3855	10
a			3876	45	3832	38	3829	39	3900	47	3910	36
b			3877	122	3833	109	3829	116	3901	142	3911	109

Table A9: Harmonic vibrational frequencies (ω) and IR intensities for the C_s Edge-Face configuration using the haTZ basis set.

	CCSD(T)		MP2		B3LYP		B3LYP-D3		ωB97XD		M06-2X	
Irrep	ω	IR Intensity	ω	IR Intensity	ω	IR Intensity	ω	IR Intensity	ω	IR Intensity	ω	IR Intensity
a''			51i	4	42i	4	57i	5	63i	1	27i	1
a'			9	1	14	1	7	1	22	1	15	1
a'			53	3	38	2	53	2	71	1	60	1
a''			64	29	50	23	61	23	74	5	58	19
a''			114	2	114	19	112	6	106	0	123	6
a'			124	0	117	1	128	0	139	1	123	0
a''			132	68	145	69	150	69	160	31	157	53
a'			141	10	130	10	146	11	161	11	140	11
a'			220	77	231	69	239	75	223	84	260	76
a''			223	0	218	0	210	0	225	55	203	21
a''			301	0	293	0	292	0	302	0	297	0
a''			304	1	295	1	297	1	313	2	305	2
a'			311	1	303	1	303	1	314	1	308	4
a''			455	6	443	3	444	3	458	30	453	4
a'			460	3	448	3	448	2	462	6	455	3
a'			462	1	451	1	452	1	471	2	461	1
a''			494	75	502	67	498	68	481	71	496	79
a'			524	63	519	50	523	29	504	89	514	79
a'			549	41	538	34	538	34	557	50	547	41
a''			551	46	539	47	540	40	558	49	549	46
a'			552	100	542	67	545	80	560	75	551	75
a'			568	7	545	54	547	56	590	8	563	9
a''			572	6	549	10	552	16	591	6	566	7
a'			732	5	707	7	709	6	755	3	728	7
a'			866	488	836	446	837	471	889	512	859	494
a''			867	405	837	405	838	405	890	418	859	415
a'			871	485	838	532	840	507	895	484	863	495
a'			1673	262	1675	231	1679	289	1671	340	1686	293
a'			1679	43	1679	75	1684	43	1677	14	1692	33
a'			3783	146	3737	201	3752	170	3842	133	3832	149
a'			3803	95	3780	86	3780	96	3847	89	3855	89
a''			3876	84	3831	75	3829	78	3901	95	3911	73
a'			3891	73	3858	56	3851	55	3907	82	3931	54

Table A10: Harmonic vibrational frequencies (ω) and IR intensities for the C_{2v} Edge-Edge configuration using the haTZ basis set.

	CCSD(T)		MP2		B3LYP		B3LYP-D3		ωB97XD		M06-2X	
Irrep	ω	IR Intensity	ω	IR Intensity	ω	IR Intensity	ω	IR Intensity	ω	IR Intensity	ω	IR Intensity
a_2	$8i$	0	$6i$	0	10	0	$9i$	0	$8i$	0	6	0
b_1	14	1	15	1	19	1	12	1	10	1	13	1
a_1	54	10	48	14	37	12	51	9	34	16	66	1
b_2	60	39	42	36	154	49	65	25	18	18	107	24
a_1	129	88	125	90	150	75	140	12	127	40	150	82
b_2	129	12	130	2	32	16	135	2	130	1	124	36
b_2	138	31	137	41	123	4	156	55	162	53	151	30
a_1	141	0	138	1	124	20	155	78	159	55	154	14
a_2	194	0	193	0	187	0	199	0	177	0	184	0
b_1	216	2	216	5	208	10	219	2	201	7	208	0
b_2	307	1	304	1	294	1	298	1	302	1	311	0
b_1	307	0	306	0	297	1	298	0	303	0	310	0
a_1	310	1	308	1	300	2	301	1	307	1	313	0
a_2	460	0	457	0	445	0	447	0	454	0	463	0
b_1	462	4	460	3	449	2	449	2	457	3	464	6
b_2	462	2	459	2	447	1	449	2	456	2	466	2
a_2	517	0	521	0	519	0	526	0	524	0	518	0
b_1	520	123	521	106	516	82	520	45	523	94	522	135
a_1	552	31	549	30	538	24	539	24	546	11	558	35
b_2	553	31	550	29	538	23	539	25	548	26	558	35
b_1	557	174	556	190	546	211	551	247	554	206	563	197
a_1	562	1	556	1	533	2	533	1	549	17	572	2
a_1	582	6	576	6	554	7	555	9	571	8	593	6
a_1	739	8	732	8	708	8	709	10	729	10	755	10
b_2	856	467	845	473	810	481	815	472	833	486	870	479
a_1	867	438	859	440	830	437	828	439	853	444	880	450
b_1	905	437	896	443	865	445	868	445	893	449	921	452
b_2	1685	185	1667	190	1671	208	1674	204	1678	209	1664	203
a_1	1698	138	1680	130	1683	123	1687	150	1691	132	1679	164
b_2	3800	67	3799	73	3767	56	3777	66	3846	62	3850	98
a_1	3801	117	3800	153	3768	187	3778	156	3847	182	3851	144
b_2	3863	57	3880	66	3840	51	3832	78	3917	61	3902	100
a_1	3867	74	3884	92	3843	73	3836	66	3921	67	3907	90

Table A11: Catersian coordinates in Angstroms (Å) for the C_{2v} Edge complex with the M06-2X method using the haTZ basis set.

Atom	x	y	z
P	0.000000	0.000000	0.476843
F	−1.613038	0.000000	0.460782
F	0.000000	1.147410	1.608850
F	0.000000	1.147435	−0.683060
F	1.613038	0.000000	0.460782
F	0.000000	−1.147435	−0.683060
F	0.000000	−1.147410	1.608850
O	0.000000	0.000000	−3.334276
H	0.000000	−0.739723	−2.716684
H	0.000000	0.739723	−2.716684

Table A12: Catersian coordinates in Angstroms (Å) for the C_{2v} Edge complex with the ωB97XD method using the haTZ basis set.

Atom	x	y	z
P	0.000000	0.000000	0.484028
F	−1.620405	0.000000	0.467697
F	0.000000	1.152388	1.621725
F	0.000000	1.154580	−0.679946
F	1.620405	0.000000	0.467697
F	0.000000	−1.154580	−0.679946
F	0.000000	−1.152388	1.621725
O	0.000000	0.000000	−3.374727
H	0.000000	−0.737632	−2.757713
H	0.000000	0.737632	−2.757713

Table A13: Catersian coordinates in Angstroms (Å) for the C_{2v} Edge complex with the B3LYP-D3 method using the haTZ basis set.

Atom	x	y	z
P	0.000000	0.000000	0.481383
F	−1.628444	0.000000	0.464898
F	0.000000	1.158106	1.624780
F	0.000000	1.160537	−0.688597
F	1.628444	0.000000	0.464898
F	0.000000	−1.160537	−0.688597
F	0.000000	−1.158106	1.624780
O	0.000000	0.000000	−3.370215
H	0.000000	−0.740545	−2.750252
H	0.000000	0.740545	−2.750252

Table A14: Catersian coordinates in Angstroms (Å) for the C_{2v} Edge complex with the B3LYP method using the haTZ basis set.

Atom	x	y	z
P	0.000000	0.000000	0.503348
F	−1.629059	0.000000	0.488290
F	0.000000	1.158579	1.646913
F	0.000000	1.159525	−0.667880
F	1.629059	0.000000	0.488290
F	0.000000	−1.159525	−0.667880
F	0.000000	−1.158579	1.646913
O	0.000000	0.000000	−3.397541
H	0.000000	−0.741664	−2.779061
H	0.000000	0.741664	−2.779061

Table A15: Catersian coordinates in Angstroms (Å) for the C_{2v} Edge complex with the MP2 method using the haTZ basis set.

Atom	x	y	z
P	0.000000	0.000000	0.482223
F	−1.620192	0.000000	0.466411
F	0.000000	1.151968	1.619761
F	0.000000	1.152906	−0.681701
F	1.620192	0.000000	0.466411
F	0.000000	−1.152906	−0.681701
F	0.000000	−1.151968	1.619761
O	0.000000	0.000000	−3.376333
H	0.000000	−0.735684	−2.751004
H	0.000000	0.735684	−2.751004

Table A16: Catersian coordinates in Angstroms (Å) for the C_{2v} Edge complex with the CCSD(T) method using the haTZ basis set.

Atom	x	y	z
O	0.000000	0.000000	0.000000
P	0.000000	0.000000	3.845824
F	1.151020	0.000000	2.684119
F	−1.151020	0.000000	2.684119
F	−1.150022	0.000000	4.981671
F	1.150022	0.000000	4.981671
F	0.000000	−1.617630	3.830200
F	0.000000	1.617630	3.830200
H	0.736611	0.000000	0.623897
H	−0.736611	0.000000	0.623897

Table A17: Catersian coordinates in Angstroms (Å) for the C_s Edge complex with the M06-2X method using the haTZ basis set.

Atom	x	y	z
P	−0.007548	−0.007644	0.049526
F	0.080974	0.082007	1.659809
F	1.601150	−0.010552	−0.050631
F	−0.030847	1.600888	−0.050631
F	−0.120759	−0.122300	−1.554678
F	−1.634877	−0.023481	0.156860
F	−0.002756	−1.635043	0.156860
O	−2.264969	−2.293864	1.865146
H	−2.434565	−1.411439	1.517006
H	−1.380465	−2.452261	1.517006

Table A18: Catersian coordinates in Angstroms (Å) for the C_s Edge complex with the ωB97XD method using the haTZ basis set.

Atom	x	y	z
P	0.027984	0.028341	0.071743
F	0.230085	0.233020	1.667279
F	1.633180	0.014088	−0.141655
F	−0.006615	1.633228	−0.141655
F	−0.197208	−0.199724	−1.516316
F	−1.596542	0.025470	0.291482
F	0.045706	−1.596091	0.291482
O	−2.358696	−2.388786	1.791120
H	−2.511468	−1.493044	1.476398
H	−1.461089	−2.530192	1.476398

Table A19: Catersian coordinates in Angstroms (Å) for the C_s Face complex with the M06-2X method using the haTZ basis set.

Atom	x	y	z
P	0.000000	0.096907	−0.367156
F	0.000000	1.646348	−0.812486
F	−1.138874	0.407917	0.744682
F	−1.144545	−0.232493	−1.453339
F	0.000000	−1.468923	0.097423
F	1.144545	−0.232493	−1.453339
F	1.138874	0.407917	0.744682
O	0.000000	−1.298131	3.007760
H	0.000000	−0.362739	2.780841
H	0.000000	−1.695107	2.128560

Table A20: Catersian coordinates in Angstroms (Å) for the C_s Face complex with the ωB97XD method using the haTZ basis set.

Atom	x	y	z
P	0.000000	−0.044688	−0.463964
F	0.000000	1.584469	−0.246131
F	−1.145656	−0.181320	0.685291
F	−1.149557	0.116314	−1.594743
F	0.000000	−1.651410	−0.668635
F	1.149557	0.116314	−1.594743
F	1.145656	−0.181320	0.685291
O	0.000000	2.099427	2.633509
H	0.000000	2.204936	1.675464
H	0.000000	1.143435	2.711143

Table A21: Catersian coordinates in Angstroms (Å) for the C_s Face complex with the B3LYP-D3 method using the haTZ basis set.

Atom	x	y	z
P	0.000000	−0.048456	−0.467798
F	0.000000	1.586548	−0.221144
F	−1.150571	−0.204731	0.683857
F	−1.154551	0.133523	−1.600694
F	0.000000	−1.659327	−0.701728
F	1.154551	0.133523	−1.600694
F	1.150571	−0.204731	0.683857
O	0.000000	2.119331	2.631281
H	0.000000	2.186581	1.665148
H	0.000000	1.163806	2.750310

Table A22: Catersian coordinates in Angstroms (Å) for the C_s Face complex with the B3LYP method using the haTZ basis set.

Atom	x	y	z
P	0.000000	−0.080385	−0.493540
F	0.000000	1.544304	−0.178670
F	−1.151306	−0.283553	0.649517
F	−1.154272	0.149359	−1.618861
F	0.000000	−1.680347	−0.794949
F	1.154272	0.149359	−1.618861
F	1.151306	−0.283553	0.649517
O	0.000000	2.221115	2.654898
H	0.000000	2.182509	1.686278
H	0.000000	1.287259	2.887068

Table A23: Catersian coordinates in Angstroms (Å) for the C_s Face complex with the MP2 method using the haTZ basis set.

Atom	x	y	z
P	0.000000	−0.041453	−0.466272
F	0.000000	1.585313	−0.238911
F	−1.144567	−0.183816	0.681520
F	−1.148632	0.125573	−1.595336
F	0.000000	−1.646499	−0.679838
F	1.148632	0.125573	−1.595336
F	1.144567	−0.183816	0.681520
O	0.000000	2.103157	2.634618
H	0.000000	2.177088	1.669573
H	0.000000	1.144947	2.730860

Table A24: Catersian coordinates in Angstroms (Å) for the C_s Face complex with the CCSD(T) method using the haTZ basis set.

Atom	x	y	z
P	0.000000	0.000000	0.000000
F	0.000000	0.000000	1.639031
H	1.824485	0.000000	2.479091
O	2.791441	0.000000	2.494819
H	2.977192	0.000000	1.549516
X	−0.999994	0.000000	−0.003327
F	0.010757	0.000000	−1.616619
F	−1.139347	−1.146939	0.008597
F	−1.139347	1.146939	0.008597
F	1.154986	−1.142632	0.017368
F	1.154986	1.142632	0.017368

Table A25: Catersian coordinates in Angstroms (Å) for the C_s WW-Edge-Face complex with the M06-2X method using the haTZ basis set.

Atom	x	y	z
P	0.754088	−0.119731	0.000000
F	1.723736	−0.690854	1.145991
F	−0.258742	0.454342	1.144745
F	−0.079071	−1.514197	0.000000
F	−0.258742	0.454342	−1.144745
F	1.723736	−0.690854	−1.145991
F	1.539648	1.284377	0.000000
O	−2.551925	1.674329	0.000000
H	−1.966612	1.484078	−0.743320
H	−1.966612	1.484078	0.743320
O	−3.049383	−1.254397	0.000000
H	−3.097885	−0.289662	0.000000
H	−2.101128	−1.432144	0.000000

Table A26: Catersian coordinates in Angstroms (Å) for the C_s WW-Edge-Face complex with the ωB97XD method using the haTZ basis set.

Atom	x	y	z
P	0.809839	−0.067170	0.000000
F	1.723079	−0.734368	1.150922
F	−0.144086	0.606133	1.152265
F	−0.158496	−1.381787	0.000000
F	−0.144086	0.606133	−1.152265
F	1.723079	−0.734368	−1.150922
F	1.734205	1.258048	0.000000
O	−2.587064	1.576616	0.000000
H	−1.989740	1.425162	−0.740193
H	−1.989740	1.425162	0.740193
O	−3.160837	−1.306047	0.000000
H	−3.189024	−0.340397	0.000000
H	−2.215925	−1.489407	0.000000

Table A27: Catersian coordinates in Angstroms (Å) for the C_s WW-Edge-Face complex with the B3LYP-D3 method using the haTZ basis set.

Atom	x	y	z
P	0.822090	−0.044881	0.000000
F	1.714092	−0.749343	1.156716
F	−0.110231	0.668247	1.158019
F	−0.199748	−1.328549	0.000000
F	−0.110231	0.668247	−1.158019
F	1.714092	−0.749343	−1.156716
F	1.800914	1.250743	0.000000
O	−2.586408	1.539942	0.000000
H	−1.981901	1.407647	−0.743254
H	−1.981901	1.407647	0.743254
O	−3.202704	−1.331382	0.000000
H	−3.208597	−0.360495	0.000000
H	−2.258264	−1.534758	0.000000

Table A28: Catersian coordinates in Angstroms (Å) for the C_s WW-Edge-Face complex with the B3LYP method using the haTZ basis set.

Atom	x	y	z
P	0.857569	−0.024137	0.000000
F	1.727654	−0.756315	1.157231
F	−0.052630	0.719188	1.157343
F	−0.204206	−1.275234	0.000000
F	−0.052630	0.719188	−1.157343
F	1.727654	−0.756315	−1.157231
F	1.878156	1.239697	0.000000
O	−2.600700	1.514073	0.000000
H	−1.993677	1.400366	−0.744220
H	−1.993677	1.400366	0.744220
O	−3.280418	−1.359882	0.000000
H	−3.259710	−0.388922	0.000000
H	−2.342194	−1.588347	0.000000

Table A29: Catersian coordinates in Angstroms (Å) for the C_s WW-Edge-Face complex with the MP2 method using the haTZ basis set.

Atom	x	y	z
P	0.825891	−0.038511	0.000000
F	1.705373	−0.750033	1.150696
F	−0.093293	0.681567	1.150680
F	−0.205829	−1.302942	0.000000
F	−0.093293	0.681567	−1.150680
F	1.705373	−0.750033	−1.150696
F	1.815560	1.238488	0.000000
O	−2.590010	1.533284	0.000000
H	−1.978662	1.406791	−0.738529
H	−1.978662	1.406791	0.738529
O	−3.216332	−1.346035	0.000000
H	−3.214670	−0.376169	0.000000
H	−2.270243	−1.541046	0.000000

Table A30: Catersian coordinates in Angstroms (Å) for the C_s WW-Edge-Face complex with the CCSD(T) method using the haTZ basis set.

Atom	x	y	z
P	0.000000	0.000000	0.000000
F	0.000000	0.000000	1.629353
H	1.461767	0.000000	3.080863
O	2.317931	0.000000	3.528019
H	2.932291	0.000000	2.778807
O	3.647917	0.000000	0.892729
X	−0.999924	0.000000	−0.012361
F	0.039876	0.000000	−1.612630
F	1.165096	−1.148763	0.022938
F	1.165096	1.148763	0.022938
F	−1.129691	−1.148780	−0.004492
F	−1.129691	1.148780	−0.004492
H	3.090624	−0.739480	0.614895
H	3.090624	0.739480	0.614895

Table A31: Catersian coordinates in Angstroms (Å) for the C_s Edge-Edge complex with the M06-2X method using the haTZ basis set.

Atom	x	y	z
P	0.139736	0.000000	−0.149739
F	−0.038730	0.000000	1.445800
F	0.340125	0.000000	−1.777554
F	1.287457	1.142657	−0.032304
F	1.287457	−1.142657	−0.032304
F	−0.979621	−1.145746	−0.304380
F	−0.979621	1.145746	−0.304380
O	0.889996	2.841802	−2.384203
O	0.889996	−2.841802	−2.384203
H	0.481160	−2.000787	−2.613133
H	0.481160	2.000787	−2.613133
H	1.133343	−2.683025	−1.465701
H	1.133343	2.683025	−1.465701

Table A32: Catersian coordinates in Angstroms (Å) for the C_s Edge-Edge complex with the ωB97XD method using the haTZ basis set.

Atom	x	y	z
P	0.061263	0.000000	−0.073331
F	−0.007521	0.000000	1.538362
F	0.155366	0.000000	−1.716520
F	1.222866	1.147615	−0.029578
F	1.222866	−1.147615	−0.029578
F	−1.070166	−1.150467	−0.150192
F	−1.070166	1.150467	−0.150192
O	1.015670	2.802691	−2.465502
O	1.015670	−2.802691	−2.465502
H	0.522097	−2.018440	−2.716199
H	0.522097	2.018440	−2.716199
H	1.237880	−2.593242	−1.553252
H	1.237880	2.593242	−1.553252

Table A33: Catersian coordinates in Angstroms (Å) for the C_s Edge-Edge complex with the B3LYP-D3 method using the haTZ basis set.

Atom	x	y	z
P	−0.001353	0.000000	−0.012579
F	0.011108	0.000000	1.608415
F	0.011316	0.000000	−1.669095
F	1.167043	1.153054	−0.027294
F	1.167043	−1.153054	−0.027294
F	−1.140425	−1.155347	−0.033398
F	−1.140425	1.155347	−0.033398
O	1.102950	2.638322	−2.560840
O	1.102950	−2.638322	−2.560840
H	0.573501	−1.855037	−2.750722
H	0.573501	1.855037	−2.750722
H	1.319297	−2.488220	−1.631585
H	1.319297	2.488220	−1.631585

Table A34: Catersian coordinates in Angstroms (Å) for the C_s Edge-Edge complex with the B3LYP method using the haTZ basis set.

Atom	x	y	z
P	−0.047926	0.000000	0.035193
F	0.039936	0.000000	1.654616
F	−0.105671	0.000000	−1.615889
F	1.120514	1.154895	−0.029979
F	1.120514	−1.154895	−0.029979
F	−1.187344	−1.155697	0.069138
F	−1.187344	1.155697	0.069138
O	1.195337	2.632186	−2.590515
O	1.195337	−2.632186	−2.590515
H	0.605770	−1.919754	−2.860676
H	0.605770	1.919754	−2.860676
H	1.355454	−2.401395	−1.665396
H	1.355454	2.401395	−1.665396

Table A35: Catersian coordinates in Angstroms (Å) for the C_s Edge-Edge complex with the MP2 method using the haTZ basis set.

Atom	x	y	z
P	0.026117	0.000000	−0.037107
F	0.002246	0.000000	1.575585
F	0.075214	0.000000	−1.682111
F	1.187625	1.147261	−0.026396
F	1.187625	−1.147261	−0.026396
F	−1.106931	−1.149915	−0.082404
F	−1.106931	1.149915	−0.082404
O	1.067237	2.710379	−2.522382
O	1.067237	−2.710379	−2.522382
H	0.551831	−1.924635	−2.737552
H	0.551831	1.924635	−2.737552
H	1.281349	−2.520748	−1.599917
H	1.281349	2.520748	−1.599917

Table A36: Catersian coordinates in Angstroms (Å) for the C_s Edge-Edge complex with the CCSD(T) method using the haTZ basis set.

Atom	x	y	z
X	0.000000	0.000000	0.000000
F	0.000000	0.000000	1.000000
P	1.643701	0.000000	1.000000
X	1.657695	0.000000	1.999902
F	3.253921	0.000000	0.977465
F	1.620075	1.145243	−0.158733
F	1.620075	−1.145243	−0.158733
F	1.631141	1.148064	2.132360
F	1.631141	−1.148064	2.132360
H	0.059973	2.549567	−0.160933
H	0.059973	−2.549567	−0.160933
O	−0.853117	2.718096	0.103114
O	−0.853117	−2.718096	0.103114
H	−1.033392	1.915805	0.606579
H	−1.033392	−1.915805	0.606579

Table A37: Catersian coordinates in Angstroms (Å) for the C_2 Edge-Edge complex with the M06-2X method using the haTZ basis set.

Atom	x	y	z
P	0.000000	0.000000	−0.110084
F	−0.832222	0.787073	1.019315
F	1.119032	1.175481	−0.119733
F	−0.826240	0.788959	−1.263712
F	0.826240	−0.788959	−1.263712
F	−1.119032	−1.175481	−0.119733
F	0.832222	−0.787073	1.019315
O	3.640857	−0.184849	−0.724557
H	2.938112	−0.762859	−1.040366
H	3.127515	0.510154	−0.298991
O	−3.640857	0.184849	−0.724557
H	−2.938112	0.762859	−1.040366
H	−3.127515	−0.510154	−0.298991

Table A38: Catersian coordinates in Angstroms (Å) for the C_2 Edge-Edge complex with the ωB97XD method using the haTZ basis set.

Atom	x	y	z
P	0.000000	0.000000	0.087084
F	−1.140663	−0.143313	1.221178
F	−0.201951	1.618589	0.076431
F	−1.138603	−0.137610	−1.073594
F	1.138603	0.137610	−1.073594
F	0.201951	−1.618589	0.076431
F	1.140663	0.143313	1.221178
O	2.277663	2.878145	−0.956107
H	2.323990	1.949414	−1.198779
H	1.456344	2.891473	−0.457046
O	−2.277663	−2.878145	−0.956107
H	−2.323990	−1.949414	−1.198779
H	−1.456344	−2.891473	−0.457046

Table A39: Catersian coordinates in Angstroms (Å) for the C_2 Edge-Edge complex with the B3LYP-D3 method using the haTZ basis set.

Atom	x	y	z
P	0.000000	0.000000	0.378119
F	−0.683787	0.930250	1.517400
F	1.320695	0.971979	0.366991
F	−0.678360	0.931482	−0.789326
F	0.678360	−0.931482	−0.789326
F	−1.320695	−0.971979	0.366991
F	0.683787	−0.930250	1.517400
O	3.409915	−0.034126	−1.440600
H	2.666094	−0.640489	−1.542786
H	3.051842	0.576260	−0.783917
O	−3.409915	0.034126	−1.440600
H	−2.666094	0.640489	−1.542786
H	−3.051842	−0.576260	−0.783917

Table A40: Catersian coordinates in Angstroms (Å) for the C_2 Edge-Edge complex with the B3LYP method using the haTZ basis set.

Atom	x	y	z
P	0.000000	0.000000	0.420600
F	−0.666665	0.942231	1.561242
F	1.338148	0.949077	0.408599
F	−0.665103	0.942122	−0.746171
F	0.665103	−0.942122	−0.746171
F	−1.338148	−0.949077	0.408599
F	0.666665	−0.942231	1.561242
O	3.419906	−0.015233	−1.496314
H	2.686832	−0.634113	−1.598895
H	3.063548	0.576799	−0.821941
O	−3.419906	0.015233	−1.496314
H	−2.686832	0.634113	−1.598895
H	−3.063548	−0.576799	−0.821941

Table A41: Catersian coordinates in Angstroms (Å) for the C_2 Edge-Edge complex with the MP2 method using the haTZ basis set.

Atom	x	y	z
P	0.000000	0.000000	0.387313
F	−0.676603	0.928108	1.521361
F	1.317574	0.961069	0.375794
F	−0.672559	0.928260	−0.773316
F	0.672559	−0.928260	−0.773316
F	−1.317574	−0.961069	0.375794
F	0.676603	−0.928108	1.521361
O	3.407585	−0.027783	−1.453469
H	2.666708	−0.637364	−1.554850
H	3.037076	0.570075	−0.792356
O	−3.407585	0.027783	−1.453469
H	−2.666708	0.637364	−1.554850
H	−3.037076	−0.570075	−0.792356

Table A42: Catersian coordinates in Angstroms (Å) for the C_2 Edge-Edge complex with the CCSD(T) method using the haTZ basis set.

Atom	x	y	z
P	0.000000	0.000000	0.000000
X	0.000000	0.000000	1.000000
F	1.628681	0.000000	0.000000
F	−1.628681	0.000000	0.000000
F	0.000000	1.149175	1.149175
F	0.000000	−1.149175	1.149175
F	0.000000	1.141502	−1.141502
F	0.000000	−1.141502	−1.141502
O	−2.747692	−1.917281	1.917281
O	2.747692	1.917281	1.917281
H	−2.769968	−1.234858	1.234858
H	2.769968	1.234858	1.234858
H	1.794282	2.019560	2.019560
H	−1.794282	−2.019560	2.019560

Table A43: Catersian coordinates in Angstroms (Å) for the C_s Edge-Face complex with the M06-2X method using the haTZ basis set.

Atom	x	y	z
P	0.764699	0.114441	0.000000
F	0.065665	1.582145	0.000000
F	−0.278936	−0.367091	1.146053
F	1.794031	0.610164	1.140911
F	1.438373	−1.346719	0.000000
F	1.794031	0.610164	−1.140911
F	−0.278936	−0.367091	−1.146053
O	−1.630285	−2.699695	0.000000
H	−1.275956	−2.199080	−0.742636
H	−1.275956	−2.199080	0.742636
O	2.365819	3.404634	0.000000
H	1.444131	3.121998	0.000000
H	2.819665	2.556230	0.000000

Table A44: Catersian coordinates in Angstroms (Å) for the C_s Edge-Face complex with the ωB97XD method using the haTZ basis set.

Atom	x	y	z
P	0.881042	0.030185	0.000000
F	0.132826	1.485127	0.000000
F	−0.154705	−0.481268	1.151949
F	1.896806	0.558288	1.147240
F	1.600432	−1.415888	0.000000
F	1.896806	0.558288	−1.147240
F	−0.154705	−0.481268	−1.151949
O	−1.862427	−2.618923	0.000000
H	−1.454406	−2.161047	−0.739982
H	−1.454406	−2.161047	0.739982
O	2.217780	3.568051	0.000000
H	1.370618	3.109793	0.000000
H	2.830690	2.830646	0.000000

Table A45: Catersian coordinates in Angstroms (Å) for the C_s Edge-Face complex with the B3LYP-D3 method using the haTZ basis set.

Atom	x	y	z
P	1.033676	−0.072751	0.000000
F	0.149667	1.314916	0.000000
F	0.043741	−0.679006	1.158321
F	2.000502	0.549985	1.152819
F	1.887064	−1.452423	0.000000
F	2.000502	0.549985	−1.152819
F	0.043741	−0.679006	−1.158321
O	−2.086897	−2.347679	0.000000
H	−1.597869	−1.971605	−0.742398
H	−1.597869	−1.971605	0.742398
O	1.984036	3.599963	0.000000
H	1.197556	3.036584	0.000000
H	2.688491	2.943665	0.000000

Table A46: Catersian coordinates in Angstroms (Å) for the C_s Edge-Face complex with the B3LYP method using the haTZ basis set.

Atom	x	y	z
P	1.095728	−0.139743	0.000000
F	0.226601	1.259567	0.000000
F	0.097335	−0.736088	1.156908
F	2.067551	0.472702	1.153857
F	1.935604	−1.528385	0.000000
F	2.067551	0.472702	−1.153857
F	0.097335	−0.736088	−1.156908
O	−2.189607	−2.277282	0.000000
H	−1.678502	−1.934227	−0.743445
H	−1.678502	−1.934227	0.743445
O	1.864635	3.704029	0.000000
H	1.173807	3.025395	0.000000
H	2.666795	3.172685	0.000000

Table A47: Catersian coordinates in Angstroms (Å) for the C_s Edge-Face complex with the MP2 method using the haTZ basis set.

Atom	x	y	z
P	1.020470	−0.058714	0.000000
F	0.138835	1.318931	0.000000
F	0.037777	−0.665522	1.151251
F	1.981083	0.563940	1.146833
F	1.874534	−1.428631	0.000000
F	1.981083	0.563940	−1.146833
F	0.037777	−0.665522	−1.151251
O	−2.078037	−2.374270	0.000000
H	−1.590201	−1.987810	−0.737538
H	−1.590201	−1.987810	0.737538
O	2.011570	3.590993	0.000000
H	1.221429	3.033451	0.000000
H	2.700223	2.918041	0.000000

Table A48: Catersian coordinates in Angstroms (Å) for the C_s Edge-Face complex with the CCSD(T) method using the haTZ basis set.

Atom	x	y	z
H	0.000000	0.000000	0.000000
O	0.000000	0.000000	0.963200
H	0.950125	0.000000	1.139744
F	2.925157	0.000000	0.644237
P	3.224284	0.000000	−0.960362
O	7.061017	0.000000	−0.648114
F	3.538237	0.000000	−2.541455
F	2.099059	−1.144867	−1.163781
F	2.099059	1.144867	−1.163781
F	4.354059	−1.149579	−0.731459
F	4.354059	1.149579	−0.731459
H	6.440595	−0.738443	−0.675622
H	6.440595	0.738443	−0.675622

Table A49: Catersian coordinates in Angstroms (Å) for the D_{2h} Edge-Edge complex with the M06-2X method using the haTZ basis set.

Atom	x	y	z
P	0.000000	0.000000	0.000000
F	0.000000	1.149254	1.146829
F	1.607913	0.000000	0.000000
F	0.000000	1.149254	−1.146829
F	0.000000	−1.149254	−1.146829
F	−1.607913	0.000000	0.000000
F	0.000000	−1.149254	1.146829
O	0.000000	0.000000	−3.818283
H	0.000000	0.741726	−3.203900
H	0.000000	−0.741726	−3.203900
O	0.000000	0.000000	3.818283
H	0.000000	0.741726	3.203900
H	0.000000	−0.741726	3.203900

Table A50: Catersian coordinates in Angstroms (Å) for the D_{2h} Edge-Edge complex with the ωB97XD method using the haTZ basis set.

Atom	x	y	z
P	0.000000	0.000000	0.000000
F	0.000000	1.156260	1.151535
F	1.615169	0.000000	0.000000
F	0.000000	1.156260	−1.151535
F	0.000000	−1.156260	−1.151535
F	−1.615169	0.000000	0.000000
F	0.000000	−1.156260	1.151535
O	0.000000	0.000000	−3.873052
H	0.000000	0.739476	−3.259137
H	0.000000	−0.739476	−3.259137
O	0.000000	0.000000	3.873052
H	0.000000	0.739476	3.259137
H	0.000000	−0.739476	3.259137

Table A51: Catersian coordinates in Angstroms (Å) for the D_{2h} Edge-Edge complex with the B3LYP-D3 method using the haTZ basis set.

Atom	x	y	z
P	0.000000	0.000000	0.000000
F	0.000000	1.161684	1.157038
F	1.622981	0.000000	0.000000
F	0.000000	1.161684	−1.157038
F	0.000000	−1.161684	−1.157038
F	−1.622981	0.000000	0.000000
F	0.000000	−1.161684	1.157038
O	0.000000	0.000000	−3.861928
H	0.000000	0.742446	−3.245082
H	0.000000	−0.742446	−3.245082
O	0.000000	0.000000	3.861928
H	0.000000	0.742446	3.245082
H	0.000000	−0.742446	3.245082

Table A52: Catersian coordinates in Angstroms (Å) for the D_{2h} Edge-Edge complex with the B3LYP method using the haTZ basis set.

Atom	x	y	z
P	0.000000	0.000000	0.000000
F	0.000000	1.160985	1.158264
F	1.623887	0.000000	0.000000
F	0.000000	1.160985	−1.158264
F	0.000000	−1.160985	−1.158264
F	−1.623887	0.000000	0.000000
F	0.000000	−1.160985	1.158264
O	0.000000	0.000000	−3.915106
H	0.000000	0.743530	−3.299656
H	0.000000	−0.743530	−3.299656
O	0.000000	0.000000	3.915106
H	0.000000	0.743530	3.299656
H	0.000000	−0.743530	3.299656

Table A53: Catersian coordinates in Angstroms (Å) for the D_{2h} Edge-Edge complex with the MP2 method using the haTZ basis set.

Atom	x	y	z
P	0.000000	0.000000	0.000000
F	0.000000	1.154377	1.151412
F	1.615267	0.000000	0.000000
F	0.000000	1.154377	−1.151412
F	0.000000	−1.154377	−1.151412
F	−1.615267	0.000000	0.000000
F	0.000000	−1.154377	1.151412
O	0.000000	0.000000	−3.869531
H	0.000000	0.737568	−3.247217
H	0.000000	−0.737568	−3.247217
O	0.000000	0.000000	3.869531
H	0.000000	0.737568	3.247217
H	0.000000	−0.737568	3.247217

Table A54: Catersian coordinates in Angstroms (Å) for the D_{2h} Edge-Edge complex with the CCSD(T) method using the haTZ basis set.

Atom	x	y	z
P	0.000000	0.000000	0.000000
X	0.000000	0.000000	1.000000
X	1.000000	0.000000	0.000000
O	−3.855551	0.000000	0.000000
O	3.855551	0.000000	0.000000
F	0.000000	0.000000	−1.612793
F	0.000000	0.000000	1.612793
F	1.149434	−1.152500	0.000000
F	1.149434	1.152500	0.000000
F	−1.149434	−1.152500	0.000000
F	−1.149434	1.152500	0.000000
H	3.234545	−0.738448	0.000000
H	3.234545	0.738448	0.000000
H	−3.234545	0.738448	0.000000
H	−3.234545	−0.738448	0.000000

Table A55: Catersian coordinates in Angstroms (Å) for the C_{2v} Edge-Edge complex with the M06-2X method using the haTZ basis set.

Atom	x	y	z
P	0.000000	0.000000	0.591561
F	0.000000	0.000000	2.197274
F	1.607797	0.000000	0.570472
F	0.000000	1.623970	0.575041
F	0.000000	0.000000	−1.050537
F	−1.607797	0.000000	0.570472
F	0.000000	−1.623970	0.575041
O	0.000000	2.746931	−2.090613
H	0.000000	2.796488	−1.128509
H	0.000000	1.793324	−2.221373
O	0.000000	−2.746931	−2.090613
H	0.000000	−1.793324	−2.221373
H	0.000000	−2.796488	−1.128509

Table A56: Catersian coordinates in Angstroms (Å) for the C_{2v} Edge-Edge complex with the ωB97XD method using the haTZ basis set.

Atom	x	y	z
P	0.000000	0.000000	0.604835
F	0.000000	0.000000	2.218070
F	1.615057	0.000000	0.585491
F	0.000000	1.633473	0.592792
F	0.000000	0.000000	−1.041263
F	−1.615057	0.000000	0.585491
F	0.000000	−1.633473	0.592792
O	0.000000	2.825765	−2.076533
H	0.000000	2.777343	−1.115342
H	0.000000	1.893227	−2.303062
O	0.000000	−2.825765	−2.076533
H	0.000000	−1.893227	−2.303062
H	0.000000	−2.777343	−1.115342

Table A57: Catersian coordinates in Angstroms (Å) for the C_{2v} Edge-Edge complex with the B3LYP-D3 method using the haTZ basis set.

Atom	x	y	z
P	0.000000	0.000000	0.603588
F	0.000000	0.000000	2.224646
F	1.622849	0.000000	0.582719
F	0.000000	1.640845	0.590400
F	0.000000	0.000000	−1.053519
F	−1.622849	0.000000	0.582719
F	0.000000	−1.640845	0.590400
O	0.000000	2.791031	−2.094488
H	0.000000	2.800008	−1.128574
H	0.000000	1.841603	−2.263247
O	0.000000	−2.791031	−2.094488
H	0.000000	−1.841603	−2.263247
H	0.000000	−2.800008	−1.128574

Table A58: Catersian coordinates in Angstroms (Å) for the C_{2v} Edge-Edge complex with the B3LYP method using the haTZ basis set.

Atom	x	y	z
P	0.000000	0.000000	0.612372
F	0.000000	0.000000	2.234135
F	1.623848	0.000000	0.595145
F	0.000000	1.642634	0.599114
F	0.000000	0.000000	−1.041449
F	−1.623848	0.000000	0.595145
F	0.000000	−1.642634	0.599114
O	0.000000	2.885437	−2.076078
H	0.000000	2.808668	−1.112464
H	0.000000	1.956991	−2.334080
O	0.000000	−2.885437	−2.076078
H	0.000000	−1.956991	−2.334080
H	0.000000	−2.808668	−1.112464

Table A59: Catersian coordinates in Angstroms (Å) for the C_{2v} Edge-Edge complex with the MP2 method using the haTZ basis set.

Atom	x	y	z
P	0.000000	0.000000	0.605251
F	0.000000	0.000000	2.218196
F	1.615156	0.000000	0.585731
F	0.000000	1.632021	0.591599
F	0.000000	0.000000	−1.040886
F	−1.615156	0.000000	0.585731
F	0.000000	−1.632021	0.591599
O	0.000000	2.806628	−2.089421
H	0.000000	2.778087	−1.123863
H	0.000000	1.862014	−2.281159
O	0.000000	−2.806628	−2.089421
H	0.000000	−1.862014	−2.281159
H	0.000000	−2.778087	−1.123863

Table A60: Catersian coordinates in Angstroms (Å) for the C_{2v} Edge-Edge complex with the CCSD(T) method using the haTZ basis set.

Atom	x	y	z
P	0.000000	0.000000	0.000000
X	0.000000	0.000000	1.000000
X	1.000000	0.000000	0.000000
X	0.000000	−1.000000	0.000000
F	−1.628719	0.000000	0.013997
F	1.628719	0.000000	0.013997
F	0.000000	1.612675	0.020015
F	0.000000	−1.612675	0.020015
F	0.000000	0.000000	−1.610471
F	0.000000	0.000000	1.644367
H	2.789449	0.000000	1.731917
H	−2.789449	0.000000	1.731917
O	2.783034	0.000000	2.697304
O	−2.783034	0.000000	2.697304
H	1.832281	0.000000	2.857084
H	−1.832281	0.000000	2.857084

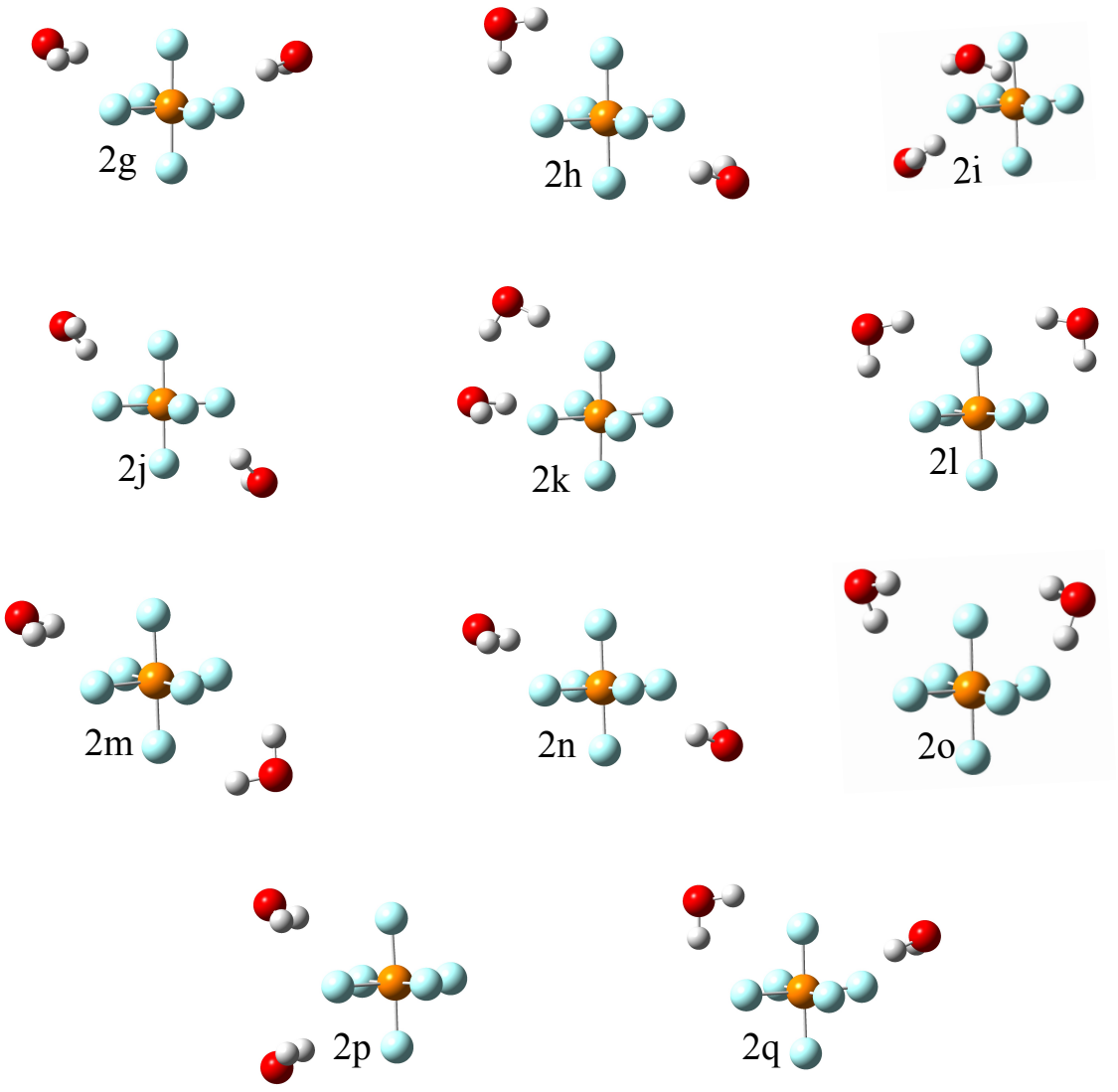

Figure A1: Low energy configurations identified as a result of the M06-2X/haTZ relaxed angular scans that collapsed to one of the configurations focused on in this study.